

BIFURCATION THEORY IN MECHANICAL SYSTEMS

Diego M. Alonso[†], Eduardo E. Paolini, and Jorge L. Moiola[†]

Dpto. de Ingeniería Eléctrica y de Computadoras
Universidad Nacional del Sur
Av. Alem 1253, B8000CPB Bahía Blanca, Argentina
[†]CONICET
e-mail: {dalonso, iepaolin, jmoiola}@criba.edu.ar

Key Words: Inverted pendulum, stabilization, bounded control, bifurcation theory, numerical continuations.

Abstract.

In this paper, bifurcation theory is used to classify different dynamical behaviors occurring in a mechanical system under bounded control actions. The example is a pendulum with an inertia disc mounted in its free extreme. By design, the control action can only be introduced by means of an external torque applied by a DC motor to the inertia disc. Imposing a bounded control action places an important obstacle to the design of a controller capable to drive the pendulum from rest to the inverted position and to stabilize it there. The only way in which the pendulum can reach the inverted position is by oscillations of increasing amplitudes. Due to the saturation of the control law the trivial equilibrium points -the rest and the inverted position- experiment a pitchfork bifurcation when one key parameter is varied. Therefore, two additional equilibrium points associated to each equilibrium of the non-forced system do appear. If another control parameter is varied, homoclinic and heteroclinic bifurcations, saddle-node bifurcations of periodic orbits, and Hopf bifurcations of equilibria do appear. Some of these codimension one bifurcations are organized in a codimension two Bogdanov-Takens bifurcation, when varying two parameters simultaneously. The application of both numerical and analytical tools from bifurcation theory to understand and classify the dynamical behavior of the closed-loop system facilitates the control law design, as shown in the paper.

1 INTRODUCTION

The stabilization of the unstable equilibrium point in pendulum-like mechanical systems is an ubiquitous problem in nonlinear control. An effective method to solve this problem is based on a *switched* strategy, using a nonlinear controller to swing-up the pendulum and switching to a linear controller to locally stabilize the pendulum at the inverted position. This strategy has been applied to a wide class of inverted pendula^{1,2,3,4}.

The stabilization with a *continuous* feedback presents serious obstacles for the controller design. Nevertheless, it has been solved for the pole-cart system⁵ and the inertia disc pendulum^{6,7}. The design of a continuous controller is hard to overcome when the amplitude of the control action is bounded. For example, Praly and co-workers⁸ addressed this problem on the inertia disc pendulum and the designed controller can not guarantee the stabilization of the inverted position when the control torque is insufficient to dominate the gravity torque. In this paper, an alternative design method is presented. The design methodology uses mathematical tools from dynamical systems theory, and specifically from bifurcation theory. After proposing a simple continuous and bounded control law⁹, both analytical and numerical methods are used to classify the different dynamical scenarios arising when control parameters are varied. It is shown that the system dynamics is organized in a codimension two or Bogdanov-Takens bifurcation when two control parameters are varied. By means of continuation of codimension one bifurcations, detected by varying one control parameter, a rather complete bifurcation diagram in a two-parameter plane is obtained. This allows to identify a region of the control parameter space where “almost” global stabilization of the pendulum at the inverted position can be achieved, *i.e.* excluding some isolated points (unstable equilibrium points) from the initial conditions, all the trajectories end up at the inverted position.

2 THE INERTIA DISC PENDULUM

The system considered is a pendulum with an inertia disc in its free extreme (see Fig. 1). The pendulum rotates freely around the pivot point, but the disc is driven by a DC motor. This mechanism belongs to the class of underactuated mechanical systems, since it has less actuators (one) than degrees of freedom (two).

The model of the inertia disc pendulum is

$$\begin{aligned}\dot{x}_1 &= x_2, \\ \dot{x}_2 &= q_1 \sin x_1 + q_2 x_3 - q_3 u, \\ \dot{x}_3 &= -q_1 \sin x_1 - q_2 (1 + \rho) x_3 + q_3 (1 + \rho) u,\end{aligned}\tag{1}$$

where x_1 is the arm position ($x_1 = 0$ at the inverted position), x_2 is the angular velocity of the arm, x_3 is the angular velocity of the disc respect to the arm, and q_1, q_2, q_3, ρ are positive parameters. The position of the inertia disc is neglected because it is irrelevant for control purposes. A more complete description of the model can be found in¹⁰.

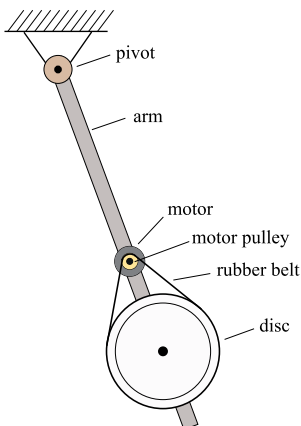


Figure 1: The inertia disk pendulum.

3 LOCAL BIFURCATION ANALYSIS

The equilibrium points of the unforced system (1) are

$$x_e = (x_{1e}, 0, 0),$$

where x_{1e} is $x_{10} = 2k\pi$ (inverted position) or $x_{1\pi} = (2k+1)\pi$ (hanging position). To avoid dealing with an infinite number of equilibria it will be assumed that x_1 belongs to S^1 , and thus only two equilibrium points are distinguishable

$$x_{00} := (x_{10}, 0, 0), \quad \text{and} \quad x_{\pi 0} := (x_{1\pi}, 0, 0),$$

corresponding to the pendulum at the inverted and the rest position, respectively, with zero velocity of the disc.

Let us consider the continuous and bounded state feedback

$$u = u_{\max} \tanh(k_1 \sin x_1 + k_2 x_2 + k_3 x_3), \quad (2)$$

where u_{\max} sets the maximum voltage applied to the motor, and k_1 , k_2 , k_3 are real feedback gains. This control law vanishes at x_{00} and $x_{\pi 0}$, and therefore the closed-loop system preserves the equilibrium points of the open-loop system.

3.1 Bifurcation analysis of x_{00} and $x_{\pi 0}$

To begin with the analysis of the closed-loop system, let us consider the linearized system at x_{00} and $x_{\pi 0}$, with the characteristic polynomials

$$P_0(s) = s^3 + a_2 s^2 + a_1 s + a_0, \quad (3)$$

and

$$P_\pi(s) = s^3 + a_2 s^2 - a_1 s - a_0, \tag{4}$$

respectively, where

$$\begin{aligned} a_0 &= \rho q_1 q_3 u_{\max} (k_3 - k_3^*), \\ a_1 &= q_3 u_{\max} (k_1 - k_1^*), \\ a_2 &= q_3 u_{\max} [k_2 - (k_3 - k_3^*) (1 + \rho)], \end{aligned}$$

and

$$k_1^* := \frac{q_1}{q_3 u_{\max}}, \quad k_3^* := \frac{q_2}{q_3 u_{\max}}.$$

Notice that by means of control gains k_1 , k_2 and k_3 all the three coefficients of the characteristic polynomials can be modified.

Bifurcations of these equilibria are studied computing the singularities of polynomials (3) and (4). In accordance to the number and type of eigenvalues of the linearized system with zero real part, five different bifurcation scenarios may arise: one eigenvalue at the origin (simple zero), a pair of imaginary eigenvalues (Hopf), a pair of eigenvalues at the origin (double zero), a pair of imaginary and a zero eigenvalues, and all the three eigenvalues at the origin (triple zero). In the following, conditions on the control parameters leading to these bifurcations are obtained.

3.1.1 A simple zero eigenvalue

A simple zero eigenvalue is the necessary condition for detecting the multiplicity of the equilibrium solution. Three elementary static bifurcations are associated with a simple zero: saddle-node, transcritical and pitchfork bifurcations. These are codimension one bifurcations since, after a reduction to the normal form, they are described by means of variations of one key parameter.

In the system under study this bifurcation occurs when $a_0 = 0$, *i.e.* when $k_3 = k_3^*$. The equilibria x_{00} and $x_{\pi 0}$ undergo a *pitchfork* bifurcation, and thus for $k_3 > k_3^*$ two symmetrical equilibrium points associated to both x_{00} and $x_{\pi 0}$ do arise. The additional equilibria are

$$x_{0+} := (x_{10}, 0, \hat{x}_{3e}), \quad x_{0-} := (x_{10}, 0, -\hat{x}_{3e}),$$

and

$$x_{\pi+} := (x_{1\pi}, 0, \hat{x}_{3e}), \quad x_{\pi-} := (x_{1\pi}, 0, -\hat{x}_{3e}),$$

where x_{3e} is the solution of

$$k_3^* x_{3e} - \tanh(k_3 x_{3e}) = 0. \tag{5}$$

Due to the symmetry of the bifurcation equation (5), the classification of the singularity is evident without the need of performing any reduction to the normal form. It is also worth mentioning that this situation frequently arises in symmetrical systems with saturations¹¹.

3.1.2 A pair of imaginary eigenvalues

A pair of imaginary eigenvalues sets the defining condition for a Hopf bifurcation. This bifurcation causes the appearance of sustained oscillations when the system's parameters move from the critical condition, *i.e.* a branch of oscillations of increasing amplitude arises depending on the value of one bifurcation parameter.

The defining condition for a Hopf bifurcation is obtained when $a_2 a_1 - a_0 = 0$, providing that $a_0 \neq 0$, $a_2 \neq 0$, and $a_1 > 0$ if the equilibrium is x_{00} , or $a_1 < 0$ if the equilibrium is $x_{\pi 0}$. In terms of the control gains this condition results

$$k_1 = k_1^* \frac{k_2 - (k_3 - k_3^*)}{k_2 - (k_3 - k_3^*)(1 + \rho)}, \quad (k_3 \neq k_3^*)$$

which is valid for $k_1 > k_1^*$ if the equilibrium analyzed is x_{00} , or for $k_1 < k_1^*$ if the equilibrium is $x_{\pi 0}$.

In the following the Hopf bifurcation of x_{00} will be referred as H1 and that of $x_{\pi 0}$ as H3. The stability of the emerging periodic solution may be determined by computing the *curvature coefficient*⁹.

3.1.3 A double zero eigenvalue

The double zero bifurcation is obtained by setting $a_0 = a_1 = 0$ and $a_2 \neq 0$, which corresponds to the control gain values

$$k_1 = k_1^*, \quad k_3 = k_3^* \quad (k_2 \neq 0).$$

Applying similarity transformations to the linearization matrices of system (1) with $k_1 = k_1^*$ and $k_3 = k_3^*$ at x_{00} and $x_{\pi 0}$, the corresponding Jordan canonical form is

$$\Lambda = \begin{pmatrix} 0 & 1 & 0 \\ 0 & 0 & 0 \\ 0 & 0 & -u_{\max} q_3 k_2 \end{pmatrix}. \quad (6)$$

This matrix has a double degeneration for $k_2 \neq 0$. Notice that for $k_2 > 0$ the eigenvalue $-u_{\max} q_3 k_2$ is contractive.

The unfolding of this codimension two singularity was performed simultaneously but independently by Takens and Bogdanov¹². Roughly speaking, this singularity introduces the dynamical phenomena of the previous bifurcations: the multiplicity of equilibrium solutions and the appearance of an oscillatory branch via the Hopf bifurcation mechanism. However, the complete characterization of the behavior of the system requires two bifurcation parameters and implies the appearance of trajectories starting and ending in the same equilibrium (homoclinic orbits) or in different equilibria (heteroclinic orbits).

3.1.4 A pair of pure imaginary eigenvalues and a simple zero

This is a codimension two bifurcation, also named Gavrilov-Guckenheimer, and occurs when $a_1 = a_2 = 0$ and $a_1 > 0$ for x_{00} and $a_1 < 0$ for $x_{\pi 0}$. This happens when the control gains take the vales

$$k_3 = k_3^*, \quad k_2 = 0,$$

providing that $k_1 > k_1^*$ for x_{00} , or $k_1 < k_1^*$ for $x_{\pi 0}$.

In this case the interactions between the multiplicity of the equilibrium solution and the oscillatory branch can lead to quasiperiodic motion and even chaotic motion in the vicinity of the singularity in the parameter plane. These complex dynamics are not examined in the present work since the main objective is the stabilization of the pendulum at the inverted position.

3.1.5 A triple zero eigenvalue

The triple zero bifurcation occurs when $a_0 = a_1 = a_2 = 0$ or

$$k_1 = k_1^*, \quad k_2 = 0, \quad k_3 = k_3^*.$$

This is a codimension three bifurcation (see matrix Λ in (6) with $k_2 = 0$) and its complete characterization is still under development¹³. However, the same comments given in the previous singularity apply here since the triple zero contains all the previous singularities as particular cases.

3.2 Bifurcation analysis of the equilibria $x_{0\pm}$ and $x_{\pi\pm}$

The characteristic polynomials at $x_{0\pm}$ and $x_{\pi\pm}$ (the additional equilibrium points that appear due to the saturated control law) are

$$P_{0\pm}(s) = s^3 + \bar{a}_2 s^2 + \bar{a}_1 s + \bar{a}_0,$$

and

$$P_{\pi\pm}(s) = s^3 + \bar{a}_2 s^2 - \bar{a}_1 s - \bar{a}_0,$$

with

$$\begin{aligned} \bar{a}_0 &= \rho q_1 q_3 u_{\max} \alpha (k_3 - k_3^*/\alpha), \\ \bar{a}_1 &= q_3 u_{\max} \alpha (k_1 - k_1^*/\alpha), \\ \bar{a}_2 &= q_3 u_{\max} \alpha (k_2 - (k_3 - k_3^*/\alpha)(1 + \rho)), \end{aligned}$$

and $\alpha := \operatorname{sech}^2(k_3 \hat{x}_{3e})$.

It can be proved that $\bar{a}_0 < 0$ for $k_3 > k_3^*$. Therefore these equilibria may only exhibit Hopf bifurcations when $\bar{a}_2\bar{a}_1 - \bar{a}_0 = 0$ provided that $a_1 > 0$ in the case of $x_{0\pm}$, or $a_1 < 0$ in the case of $x_{\pi\pm}$. In terms of control gains this results in

$$k_1 = \frac{k_1^*}{\alpha} \frac{k_2 - (k_3 - k_3^*/\alpha)}{k_2 - (k_3 - k_3^*/\alpha)(1 + \rho)},$$

and provided that $k_2 > 0$, only $x_{\pi\pm}$ can exhibit Hopf bifurcations. In the following this bifurcation will be referred to as H2.

4 LOCAL BEHAVIOR: STABILIZATION AT THE INVERTED POSITION

The main objective of the analysis of the system dynamics is to find values for the control gains assuring the stabilization of the pendulum at the inverted position x_{00} . By applying standard stability tests such as the Routh-Hurwitz criterion, it is possible to achieve the local asymptotic stability of x_{00} when the control gains do satisfy

$$\begin{aligned} k_3 &> k_3^*, \\ k_2 &> (1 + \rho)(k_3 - k_3^*), \\ k_1 &> k_1^* \frac{k_2 - (k_3 - k_3^*)}{k_2 - (1 + \rho)(k_3 - k_3^*)}. \end{aligned} \quad (7)$$

Notice that (7) implies that k_1 , k_2 and k_3 must be positive.

To analyze the stability of the remaining equilibria, let us consider the parameter plane $k_1 - k_3$ by fixing k_2 at some positive value. Then, applying conventional stability tests, five different scenarios arise as depicted in Fig. 2. The stability of the six physically distinguishable equilibrium points in each of these cases is shown in Table 1.

Notice that in zone I the only stable equilibrium point is x_{00} , *i.e.* the inverted position. Therefore, if no other attractor exists for k_1 and k_3 in this zone, the stabilization of the pendulum at the inverted position can be achieved.

In the following Section the *global* dynamical behavior of the system is addressed in order to classify other bifurcations which can not be detected by the local stability analysis of the equilibria. These additional bifurcations are homoclinic and heteroclinic connections and bifurcations of the limit cycles appearing via the Hopf mechanism.

5 GLOBAL BEHAVIOR: NUMERICAL STUDY

The bifurcation of higher codimension considered in this paper is the double-zero or Bogdanov-Takens bifurcation. In a small neighborhood of x_{00} or $x_{\pi 0}$, the system behavior may be analyzed by reducing the dynamics to the center manifold associated to this singularity. Nevertheless, to perform the analysis over a larger domain the whole nonlinear system should be considered. For this reason the analysis is performed numerically using the continuation package XPP-AUTO¹⁴.

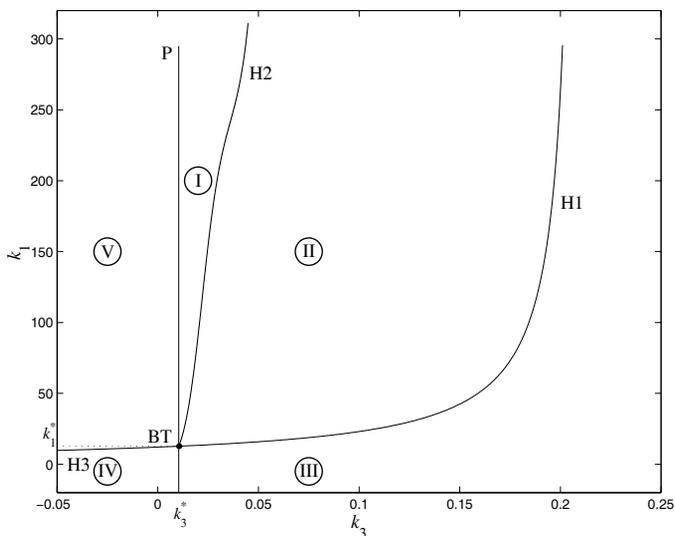


Figure 2: Zones in the parameter space with different stability of the equilibrium points ($k_2 = 50$). H1, H2 and H3 are Hopf bifurcation curves, P is a pitchfork bifurcation (simple zero) and BT is the condition for the Bogdanov-Takens bifurcation (double zero).

Zone	x_{00}	$x_{\pi 0}$	$x_{0\pm}$	$x_{\pi\pm}$
I	S	U	U	U
II	S	U	U	S
III	U	U	U	S
IV	U	S	-	-
V	U	U	-	-

Table 1: Stability of the equilibrium points in the parameter plane $k_1 - k_3$ when $k_2 = 50$. See zones I-V in Fig. 2

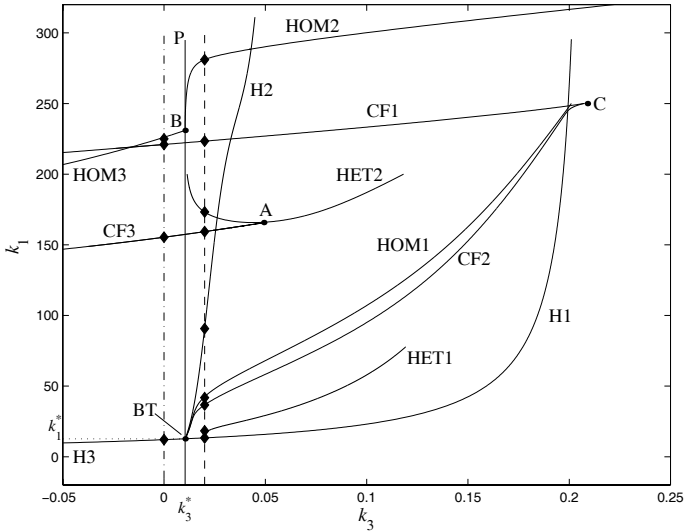


Figure 3: Numerical unfolding of the Bogdanov-Takens bifurcation.

For the numerical study of the system behavior the following parameter values were used: $q_1 = 30$, $q_2 = 0.0245$, $q_3 = 0.0393$, $\rho = 250$; the bound on the control amplitude was fixed at $u_{\max} = 60$. Since the Bogdanov-Takens bifurcation occurs at the point $k_1 = k_1^* = 12.7226$ and $k_3 = k_3^* = 0.01039$ for $k_2 \neq 0$, the control gain k_2 was fixed arbitrarily at $k_2 = 50$. As it will be shown, this codimension two point acts as an organizing centre for the dynamics when k_2 is fixed.

The unfolding of this codimension two bifurcation is depicted in Fig. 3. For $k_3 < k_3^*$ only two equilibrium points do exist: the rest position x_{π_0} and the inverted position x_{00} ; for $k_3 > k_3^*$ six equilibria do exist due to the pitchfork bifurcation (P). Simulation results allow us to conjecture on the existence of a bidimensional manifold where all the qualitative changes of the dynamics take place. The equilibrium points for $k_3 > k_3^*$ on this manifold are depicted in Fig. 4 where the stability may change depending on the parameter values. Notice that the segments A-A' and B-B' are homologues since the state variable x_1 is periodic.

Let us consider $k_3 = 0.02$ (see the dashed line in Fig. 3). The different behaviors obtained when k_1 is varied are shown in Fig. 5 where the period of the limit cycles is plotted against parameter k_1 . Beginning at the left, the first detected phenomenon is a Hopf bifurcation (H1) experimented by x_{00} when $k_1 = 13.365$ (see also the curve H1 in Fig. 3). The equilibrium point x_{00} changes the stability from unstable to stable as

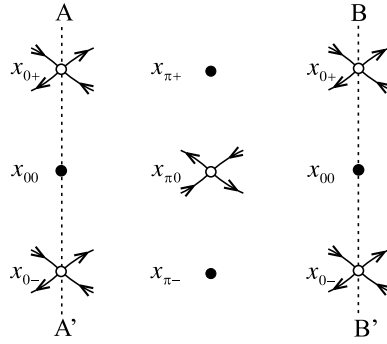


Figure 4: Equilibrium points for $k_3 > k_3^*$.

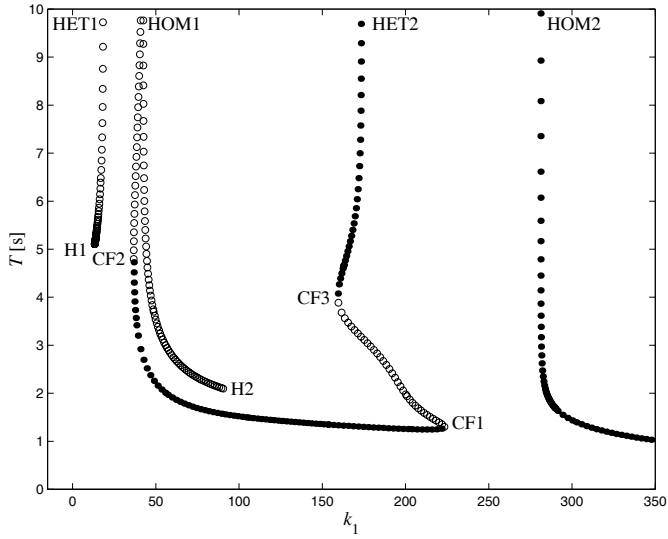


Figure 5: Continuation curves for $k_3 = 0.02$ ($k_2 = 50$). (●) Stable limit cycles; (○) unstable limit cycles.

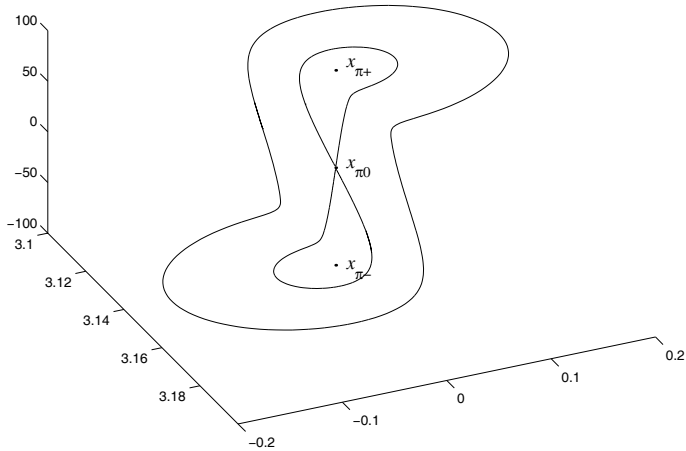


Figure 6: Limit cycles obtained with $k_1 = 42.5358$, $k_2 = 50$ and $k_3 = 0.02$.

k_1 passes through this critical value. In addition, an unstable limit cycle arises. The amplitude of this cycle grows until it collides with x_{0+} and x_{0-} for $k_1 = 18.303$ leading to an heteroclinic bifurcation (or homoclinic cycle). At this point the unstable manifold of x_{0+} is connected to the stable manifold of x_{0-} , and conversely. Notice that the period of this cycle grows asymptotically to infinity.

A second local phenomena is a Hopf bifurcation (H2) experimented by $x_{\pi+}$ and $x_{\pi-}$ at $k_1 = 90.699$. For $k_1 < 90.699$, $x_{\pi+}$ and $x_{\pi-}$ are stable and they are surrounded by antisymmetric unstable limit cycles. These cycles do collide with the equilibrium point $x_{\pi0}$ at $k_1 = 41.809$ when a double saddle connection or homoclinic bifurcation occurs (HOM1). The typical eight figure is shown in Fig. 6. For $k_1 < 41.809$ both cycles form an unique unstable cycle which coalesces with the stable one at $k_1 = 36.700$. For $k_1 = 159.331$ a cyclic fold bifurcation (CF3) occurs. A stable and unstable cycles do arise for $k_1 > 159.331$. The stable one coalesce in an heteroclinic bifurcation (HET2) when $k_1 = 173.228$, while the unstable one coalesce in a cycle fold (CF1) at $k_1 = 223.386$.

Finally, an homoclinic bifurcation (HOM2) occurs for $k_1 = 281.069$. Beyond this value a stable cycle arises, corresponding to rotations of the pendulum around the pivot point.

Now, let us consider $k_3 = 0$ (dash and dot line in Fig. 3). Since $k_3 < k_3^*$ the equilibrium points are x_{00} and $x_{\pi0}$ only. The bifurcation diagram, obtained varying k_1 , is shown in Fig. 7. The equilibrium point $x_{\pi0}$ exhibits a Hopf bifurcation for $k_1 = 12.0945$ and a stable limit cycle appears for increasing values of k_1 . For $k_1 = 155.385$ a cyclic fold bifurcation

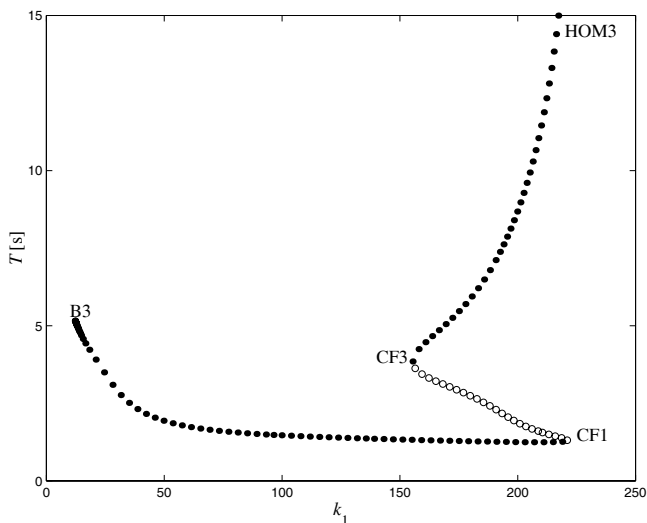


Figure 7: Continuation curves for $k_3 = 0$ ($k_2 = 50$). (●) Stable limit cycles; (○) unstable limit cycles.

(CF3) occurs and a stable and unstable cycles do appear and thus three cycles coexist for higher values of k_1 . The stable cycle undergoes an homoclinic bifurcation at $k_1 = 225$, since it reaches the equilibrium point x_{00} , and it is destroyed by this bifurcation. Finally, the remaining unstable and stable cycles coalesce in a cyclic fold bifurcation (CF1) at $k_1 = 221.032$.

The described bifurcations are all of codimension one, and by numerical continuation of these points the full picture of Fig. 3 is obtained. Notice from this figure that curves H1, HET1, CF2, HOM1, H2 and P converge to the point $k_1 = k_1^*$ and $k_3 = k_3^*$, *i.e.* the Bogdanov-Takens bifurcation BT. It is important to mention that the continuation of heteroclinic bifurcations HET1 and HET2 are very difficult to compute due to numerical problems. HET2 could only be continued partially, and the curve HET1 has been obtained by continuing a cycle of a large period, near the bifurcation, instead of continuing the true heteroclinic bifurcation.

The homoclinic cycle formed at the bifurcation HET2 change its stability at the point A where the cyclic fold bifurcation CF3 meets the curve HET2. This is a global phenomena which can not be described by the local analysis of the Bogdanov-Takens bifurcation, and corresponds to the unfolding of a higher codimension bifurcation. Two other distinctive points are worth mentioning. Point B appears at the confluence of four curves: the pitchfork P and the homoclinic and heteroclinic HOM3, HOM2 and HET2. The point C is a cusp of cyclic fold bifurcations.

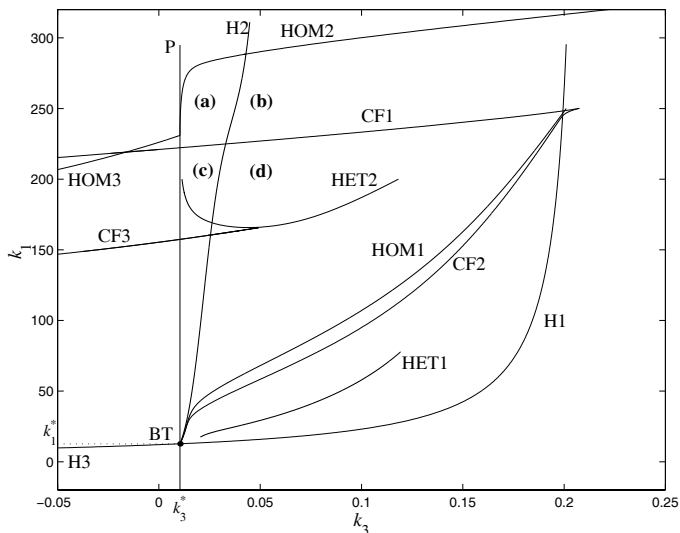


Figure 8: In zone (a) the equilibrium x_{00} (inverted position) is the unique attractor of the system. See the phase portraits of Fig. 9.

6 “ALMOST” GLOBAL STABILIZATION AT THE INVERTED POSITION

An important result from the numerical study is that for k_1 and k_3 in the region named (a) in Fig. 8 the equilibrium point x_{00} is the unique attractor of the system and thus the asymptotic stabilization of the pendulum at the inverted position is obtained. Figure 9a shows the qualitative behavior in this region (provided that trajectories are reduced to the invariant manifold).

Crossing the curve H2 in Fig. 8 from left to right, the equilibria $x_{\pi+}$ and $x_{\pi-}$ undergo a Hopf bifurcation, they become stable and two unstable limit cycles do arise, restricting the domain of attraction of x_{00} . This situation is depicted in Fig. 9b.

In region (c) a pair of limit cycles of opposed stability appear due to the cyclic fold bifurcation CF1. This bifurcation drastically reduces the basin of attraction of x_{00} (see Fig. 9c). When crossing the curve H2 towards region (d), two additional small antisymmetric cycles surrounding $x_{\pi+}$ and $x_{\pi-}$ (depicted in Fig. 9d) do appear.

Finally, a numerical simulation for values of control gains lying inside region (a) of Fig. 8 ($k_1 = 250$, $k_3 = 0.02$, $k_2 = 50$) is shown in Fig. 10. The simulation is started near the rest position, at $x = (\pi, 0, -1)$ and after a series of oscillations of increasing amplitude the pendulum is stabilized at the inverted position.

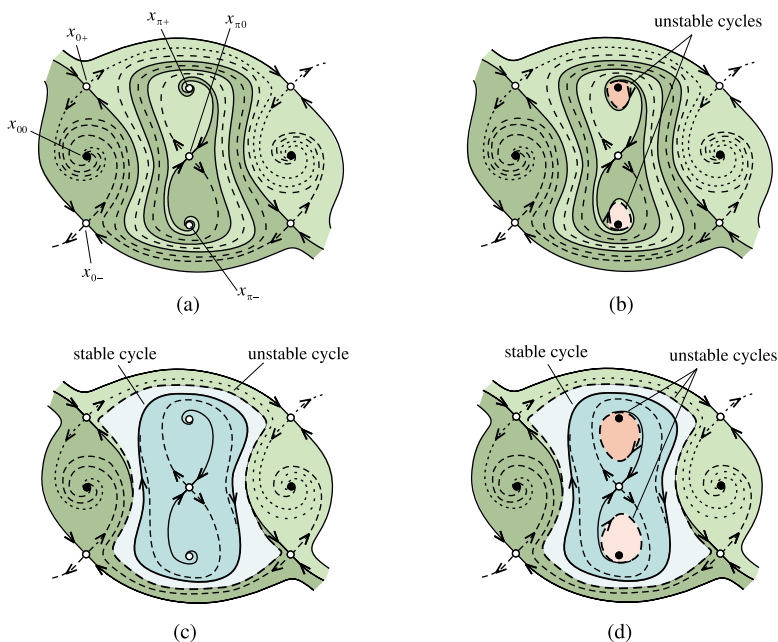


Figure 9: Phase portraits in the two dimensional manifold for parameter values in regions (a), (b), (c) and (d) in Fig. 8.

7 CONCLUSIONS

In this paper, tools from bifurcation theory have been applied to obtain proper feedback gains values for the stabilization of a pendulum-like mechanical system at the inverted position. A local analytical bifurcation study has been performed and a rather complete bifurcation diagram in two parameters have been presented. The dynamics is organized in a codimension two bifurcation, more precisely in a Bogdanov-Takens bifurcation with a special symmetry. From the bifurcation analysis, a region in the parameter space assuring “almost” global stabilization of the pendulum at the inverted position has been detected and illustrated with simulations.

REFERENCES

- [1] K. J. Åström and K. Furuta. Swinging up a pendulum by energy control. In *Proc. 13th IFAC World Congress*, pages 37–42, San Francisco, USA, (1996).

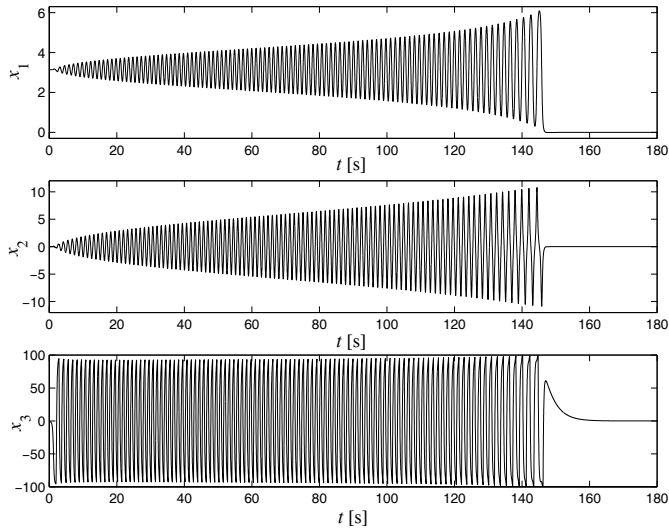


Figure 10: Evolution of the states of the system for control gains $k_1 = 250$, $k_2 = 50$ and $k_3 = 0.02$. The initial condition is $x = (\pi, 0, -1)$ and at $t \approx 150$ s the pendulum is stabilized at the inverted position.

- [2] R. Lozano, I. Fantoni, and D. Block. Stabilization of the inverted pendulum around its homoclinic orbit. *Systems & Control Letters*, **40**, 197–204 (2000).
- [3] A. Shiriaev, A. Pogromsky, H. Ludvigsen, and O. Egeland. On global properties of passivity-based control of an inverted pendulum. *Int. J. Robust Nonlinear Control*, **10**, 283–300 (2000).
- [4] M. W. Spong, P. Corke, and R. Lozano. Nonlinear control of the reaction wheel pendulum. *Automatica*, **37**(11), 1845–1851 (2001).
- [5] D. Angeli. Almost global stabilization of the inverted pendulum via continuous state feedback. *Automatica*, **37**, 1103–1108 (2001).
- [6] R. Ortega and M. Spong. Stabilization of underactuated mechanical systems via interconnection and damping assignment. In *Proc. IFAC Workshop on Lagrangian and Hamiltonian Methods in Nonlinear Systems*, Princeton, USA, (2000).
- [7] R. Olfati-Saber. Global stabilization of a flat underactuated system: the inertia wheel pendulum. In *Proc. 40th IEEE Conf. on Decision and Control (CDC'01)*, pages 3764–3765, Orlando, USA, (2001).
- [8] L. Praly, R. Ortega, and G. Kaliora. Stabilization of nonlinear systems via forwarding $\text{mod}\{L_g V\}$. *IEEE Trans. on Automatic Control*, **49**(9), 1461–1466 (2001).
- [9] D. M. Alonso, E. E. Paolini, and J. L. Moiola. Controlling an inverted pendulum with bounded controls. In L. Gruene and F. Colonius, editors, *Dynamics, Bifurcations, and*

- Control*, volume 273 of *Lecture Notes in Control and Information Sciences*, pages 3–16. Springer-Verlag, Berlin, (2002).
- [10] D. M. Alonso, E. E. Paolini, and J. L. Moiola. Experimental application of the anticontrol of Hopf bifurcations. *Int. J. of Bifurcation and Chaos*, **11**(7), 1977–1987 (2001).
- [11] M. G. Ortega, J. Aracil, F. Gordillo, and F. Rubio. Bifurcation analysis of a feedback system with dead zone and saturation. *IEEE Control Systems Magazine*, **20**(4), 91–101 (2000).
- [12] J. Guckenheimer and P. Holmes. *Nonlinear Oscillations, Dynamical Systems, and Bifurcations of Vector Fields*. Springer Verlag, New York, (1993).
- [13] A. Algaba, E. Freire, E. Gamero, and A. J. Rodríguez-Luis. On a codimension-three unfolding of the interaction of degenerate Hopf and pitchfork bifurcations. *Int. J. of Bifurcation and Chaos*, **9**(7), 1333–1362 (1999).
- [14] B. Ermentrout. XPPAUT5.0 - the differential equations tool (Available from: www.pitt.edu/~phase/). Technical report, University of Pittsburgh, Pittsburg, USA, (2001).